

## Analytical approach to the mean-return-time phase of isotropic stochastic oscillators

Konstantin Holzhausen<sup>1,2</sup>, Peter J. Thomas<sup>3</sup>, and Benjamin Lindner<sup>1,2</sup>

<sup>1</sup>*Bernstein Center for Computational Neuroscience Berlin, Philippstr. 13, Haus 2, 10115 Berlin, Germany*

<sup>2</sup>*Physics Department of Humboldt University Berlin, Newtonstr. 15, 12489 Berlin, Germany*

<sup>3</sup>*Department of Mathematics, Applied Mathematics and Statistics, 212 Yost Hall, Case Western Reserve University, 10900 Euclid Avenue, Cleveland, Ohio, USA*



(Received 13 August 2021; accepted 24 January 2022; published 8 February 2022)

One notion of phase for stochastic oscillators is based on the mean return-time (MRT): a set of points represents a certain phase if the mean time to return from any point in this set to this set after one rotation is equal to the mean rotation period of the oscillator (irrespective of the starting point). For this so far only algorithmically defined phase, we derive here analytical expressions for the important class of isotropic stochastic oscillators. This allows us to evaluate cases from the literature explicitly and to study the behavior of the MRT phase in the limits of strong noise. We also use the same formalism to show that lines of constant return time variance (instead of constant mean return time) can be defined, and that they in general differ from the MRT isochrons.

DOI: [10.1103/PhysRevE.105.024202](https://doi.org/10.1103/PhysRevE.105.024202)

### I. INTRODUCTION

Oscillatory processes encountered in physics and biology often come along with a substantial component of randomness and are then termed *stochastic oscillations*. Intracellular calcium waves [1], neural action potentials [2], rhythmic fluctuations in lasing intensity [3], and population oscillations of prey-predator systems [4] all show pronounced fluctuations in their amplitude as well as in the timing of the cycles.

In order to find a reduced description of such random oscillations, in recent years efforts have been made to generalize the phase concept for deterministic oscillators [5,6] (which has also been applied to systems with weak noise, see, e.g., Refs. [7–10]) to the stochastic case [11] (see also Refs. [12–16]). The first proposal, the mean–return-time (MRT) phase by Schwabedal and Pikovsky [11], is an intuitive generalization of the stroboscopic return-time-phase definition for deterministic oscillators: in the two-dimensional case, with any starting point on the line of equal phase (isochron), the mean return-time to the very same line after one rotation is equal to the mean rotation period of the oscillator. Schwabedal and Pikovsky suggested an algorithmic procedure to deform a line until (experimental or simulated) data satisfy this criterion. Cao *et al.* [17] showed more recently, that the MRT phase for planar white-Gaussian noise-driven oscillators obeys a partial differential equation with an unusual jump condition.

Based on Ref. [17] we present an analytical solution for the MRT phase for the important class of isotropic stochastic oscillators. The solution is given in terms of quadratures and is exploited to explore the limit of strong noise and the role of boundaries for so-far purely numerically treated examples from the literature. Finally, our approach allows us to go beyond the familiar notion of isochrons (lines of constant mean rotation time) to introduce a new construct, the *isovariance* lines (lines of constant variance of the rotation time). We demonstrate that the isovariance lines strongly differ from the isochrons.

### II. MODEL AND METHODS

We consider a class of rotationally invariant planar stochastic oscillators (also called isotropic stochastic oscillators) that obey

$$\begin{aligned}\dot{\rho} &= g(\rho) + q_\rho(\rho) \xi_\rho(t), \\ \dot{\phi} &= f(\rho) + q_\phi(\rho) \xi_\phi(t),\end{aligned}\quad (1)$$

in polar coordinates, where  $\xi_{\rho,\phi}$  denote white-Gaussian noise sources with  $\langle \xi_i(t) \xi_j(t') \rangle = \delta_{i,j} \delta(t - t')$ ,  $i, j \in \{\rho, \phi\}$ . If the noise is multiplicative ( $q_\rho(\rho) \neq \text{const}$ ) we interpret it in the sense of Ito [18]. We impose reflecting boundaries at an inner circle with radius  $\rho_-$  and an outer circle  $\rho_+$  such that the dynamics is restricted to  $\rho_- < \rho(t) < \rho_+$ . We assume that there is a mean rotation around the origin, the rotational sense of which may change depending on the parameters.

Because none of the functions on the right-hand side depend explicitly on the phase  $\phi$ , the stochastic dynamics is rotationally invariant, which is why we refer to Eq. (1) as an isotropic oscillator. In particular, we expect that the isochrons for different phases  $\psi \in [0, 2\pi]$  will be rotationally invariant as well, and can be expressed via  $\varphi(\rho) = \phi_1(\rho) + \psi$ . In the following we calculate  $\phi_1(\rho)$ .

#### A. Derivation of the isochron expression

According to Ref. [17], the MRT isochrons are the level sets of a mean-first-passage-time function  $T(\rho, \phi)$ . Given a curve in our two-dimensional domain as a simple connection between the inner boundary at  $\rho_-$  and the outer boundary at  $\rho_+$ , we can ask how long it takes the oscillator to return to this curve *after having completed one rotation*. This time is a random variable the mean value of which will, in general, depend on the starting point  $(\rho, \phi)$  on the considered curve. The family of curves for which the mean value of the return

time *does not depend* on the starting point constitutes the MRT phase isochrons.

The mean-first-passage-time function is the solution to the partial differential equation

$$\mathcal{L}^\dagger T(\rho, \phi) = \left[ g\partial_\rho + f\partial_\phi + \frac{q_\rho^2}{2}\partial_\rho^2 + \frac{q_\phi^2}{2}\partial_\phi^2 \right] T(\rho, \phi) = -1. \quad (2)$$

$\mathcal{L}^\dagger$  is the adjoint of the Kolmogorov forward operator, i.e., the operator associated with the so-called backward Fokker-Planck equation [18]. Reflecting boundary conditions for the forward equation imply the following adjoint boundary conditions for  $T(\rho, \phi)$  (cf. Ref. [18], Sec. 5.2.4)

$$q_\rho^2 \partial_\rho T(\rho, \phi) \Big|_{\rho=\rho_\pm} = 0. \quad (3)$$

In addition to that,  $T(\rho, \phi)$  satisfies a periodic-plus-jump condition at an arbitrary connection between the inner and outer boundaries (here we choose for simplicity the line  $\phi = 0$  and consider a counterclockwise rotation):

$$T(\rho, 2\pi) + \bar{T} = T(\rho, 0). \quad (4)$$

$\bar{T}$  denotes the mean period, the time it takes one realization of the process on average to perform one revolution around the origin. Following Ref. [17], we assume  $f, g, q_\rho, q_\phi \in \mathcal{C}^2$  as well as  $q_\rho^2(\rho) > 0$  and  $q_\phi^2(\phi) > 0$  for all  $\rho \in [\rho_-, \rho_+]$ . The choice of polar coordinates translates the rotational invariance of Eq. (1) into a translational invariance in the angular coordinate  $\phi$ . Correspondingly, a symmetry-adapted solution is of the general form

$$T(\rho, \phi) = -\frac{\bar{T}}{2\pi} \phi + T_\rho(\rho) \quad (5)$$

that also fulfills the periodic-plus-jump condition. This symmetry-adapted ansatz reduces the number of dimensions in Eq. (2), giving an ordinary differential equation for  $T_\rho$  in  $\rho$ , which can be solved explicitly in terms of quadratures. The isochron  $\phi_I$  as a special level set of  $T(\rho, \phi)$  can then be parametrized according to  $\phi_I(\rho) = 2\pi T_\rho(\rho)/\bar{T}$ , leading to our main result:

$$\phi_I(\rho) = 2 \int_{\rho_-}^{\rho} dq \int_{\rho_-}^q du \frac{f(u) - \bar{\omega}}{q_\rho^2(u)} \exp \left[ -2 \int_u^q dv \frac{g(v)}{q_\rho^2(v)} \right]. \quad (6)$$

The mean rotation frequency  $\bar{\omega}$  (essentially, the inverse mean rotation period  $2\pi/\bar{T}$ ) is given by

$$\bar{\omega} = \frac{2\pi}{\bar{T}} = \frac{\int_{\rho_-}^{\rho_+} d\rho f(\rho)/q_\rho^2(\rho) e^{-2 \int_{\rho_-}^{\rho_+} d\rho' q_\rho^{-2}(\rho') g(\rho')}}{\int_{\rho_-}^{\rho_+} d\rho q_\rho^{-2}(\rho) e^{-2 \int_{\rho_-}^{\rho_+} d\rho' q_\rho^{-2}(\rho') g(\rho')}}. \quad (7)$$

We can make a few conclusions from the analytical result Eq. (6) without any numerical evaluation: (i)  $q_\phi$ , i.e., the strength of phase diffusion, does not enter the isochron parametrization at all (all oscillators that only differ with respect to  $q_\phi$  have the same isochrons); (ii) the slope of the phase  $d\phi/d\rho$  is given by the difference between the local phase progression speed  $f(\rho)$  and the average speed  $\bar{\omega}$  weighted with the (normalized) steady state density of the radius and averaged over the interval  $(\rho_-, \rho)$ ; (iii) if the overall strength of the radial noise increases without bounds and we keep the two boundary values  $\rho_\pm$  fixed at nonvanishing finite values,

the integrand in Eq. (6) approaches zero, i.e., the isochron  $\phi_I$  does not depend on the radius anymore and isochrons approach the shape of spokes of a wheel.

## B. Simulation methods

We validate our analytic findings by measuring the mean rotation time  $\bar{T}$  and testing the MRT phase isochrons for their defining property in numerical simulations. The Itô equations are solved using the Euler-Maruyama method with a time step of  $\Delta t = 10^{-4}$ , taking the reflecting boundaries of the domain into account.  $\bar{T}$  is a stationary property that is inferred from the trajectories of the unwrapped phase  $\phi(t)$  by

$$\bar{T} = 2\pi \frac{t_{\text{final}} - t_{\text{start}}}{\phi(t_{\text{final}}) - \phi(t_{\text{start}})} \quad (8)$$

at long simulation times  $t_{\text{final}} - t_{\text{start}} = 10^5$ . To test the isochron property, the first return times  $T(\rho_0)$  are measured for different initial positions  $(\rho_0, \phi_I(\rho_0))$  along the isochron across an ensemble consisting of  $N = 10^5$  realizations. The system is simulated on an extended domain  $[\rho_-, \rho_+] \times \mathbb{R}$  which allows the angular coordinate  $\phi$  to take any real value. On that domain the same isochron is repeatedly represented, representations being separated by  $2\pi$  in  $\phi$ . In this setup, a return event corresponds to a first passage from  $(\rho_0, \phi_I(\rho_0))$  to the curve  $(\rho, \phi_I(\rho) + 2\pi)$  (if the mean rotation is mathematically positive) or to the curve  $(\rho, \phi_I(\rho) - 2\pi)$  (if the mean rotation is mathematically negative); this condition ensures that the system has rotated once around the origin. The mean return times are calculated as the first moments of the return time distribution in the ensemble  $\langle T(\rho_0) \rangle$ . In a similar fashion, we can also compute the variances of the return times  $\langle \Delta T^2(\rho_0) \rangle$  for starting points on the so-called iso-variance curves (see Sec. IV). A related calculation of the variance of the return time was obtained by Ref. [19] in the small-noise limit.

## III. SPECIFIC EXAMPLES

We now turn to different examples for rotationally symmetric stochastic oscillators and study the structure of the isochrones.

### A. Newby-Schwemmer oscillator

This is given by Ref. [20]

$$\begin{aligned} \dot{\rho} &= -\gamma \rho (\rho^2 - 1) + \frac{D}{\rho} + \sqrt{2D} \xi_\rho(t), \\ \dot{\phi} &= \omega + \omega \gamma c (1 - \rho)^2 + \frac{\sqrt{2D}}{\rho} \xi_\phi(t). \end{aligned} \quad (9)$$

The sense of rotation is counterclockwise on the limit cycle at  $\rho = 1$  but, for  $c < 0$ , turns to clockwise when the trajectory deviates sufficiently both towards the inside and the outside. With noise, the occupation probability w.r.t.  $\rho$  determines whether the net rotation goes clockwise or counterclockwise [20], and at the transition point  $D = D_t$  between both regimes, the mean rotation time diverges [see Fig. 1(c)].

The deterministic isochron [dark green line in Figs. 1(a) and 1(b)] has a hooklike shape, because points away from

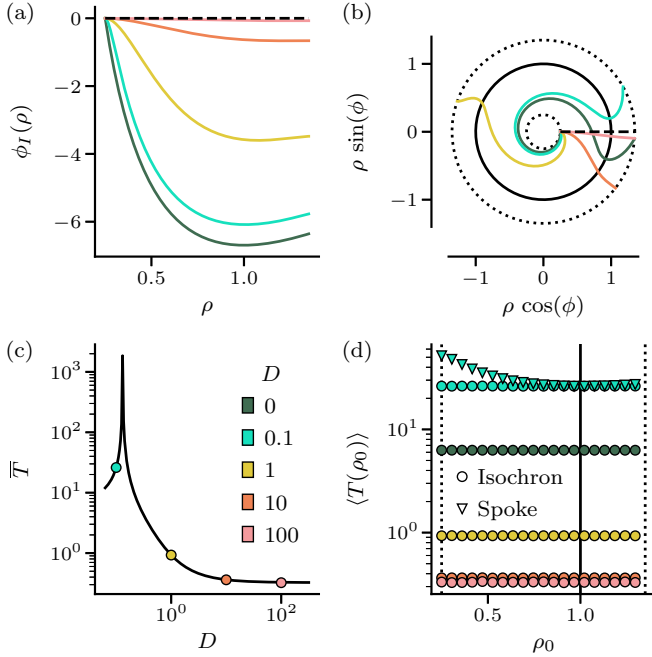


FIG. 1. MRT-Isochrons of the Newby-Schwemmer model. (a) Isochron parametrization  $\phi_I(\rho)$ , Eq. (6). (b) Isochrons (colored), reflecting boundaries (dotted) and limit cycle (solid black) [isochrons for different  $D$  are arbitrarily aligned to start at  $\phi = 0$  on the inner boundary  $\rho_-$ ]. (c) Mean period  $\bar{T}$  vs  $D$  according to theory (lines) and simulations (circles). (d) Mean return-time  $\langle T(\rho_0) \rangle$  to a curve vs initial position  $\rho_0$  on this curve, for the curve being an isochron (circles, different colors represent different  $D$ ) or a spoke (triangles, here  $D = 0.1$ ).

the limit cycle need some head start (net rotation is counterclockwise). For nonvanishing noise this principal shape is maintained: for  $D < D_t$  the net rotation is still counterclockwise, and points off the limit cycle need a headstart; for  $D > D_t$  these points need a “later” start (net rotation is clockwise), thus the isochron has the same curvature. In addition, with increasing noise intensity  $D$  the isochrons become flatter, approaching the spoke of a wheel (dashed black line) as predicted by our general conclusion (iii) above.

We checked the constant-MRT property by performing extensive simulations with ensembles of stochastic trajectories for a certain noise intensity  $D$  starting on the corresponding isochron. Indeed, the MRT for a given noise intensity from and to the isochron do not depend on the specific starting point along the isochron [circles in Fig. 1(d)]. In marked contrast, choosing (for a comparatively small noise intensity) as initial set and target line the spoke of a wheel, the mean return times do depend on the initial position [triangles in Fig. 1(d)].

### B. Guckenheimer-Schwabedal-Pikovsky oscillator

A classic example of a deterministic system, in which the definition of phase is problematic, is one with two limit cycles with distinct rotation frequencies (this example goes back to Guckenheimer [6]). As shown numerically by Schwabedal and Pikovsky [11], with noise, transitions occur between the attraction domains of the two limit cycles and thus the MRT

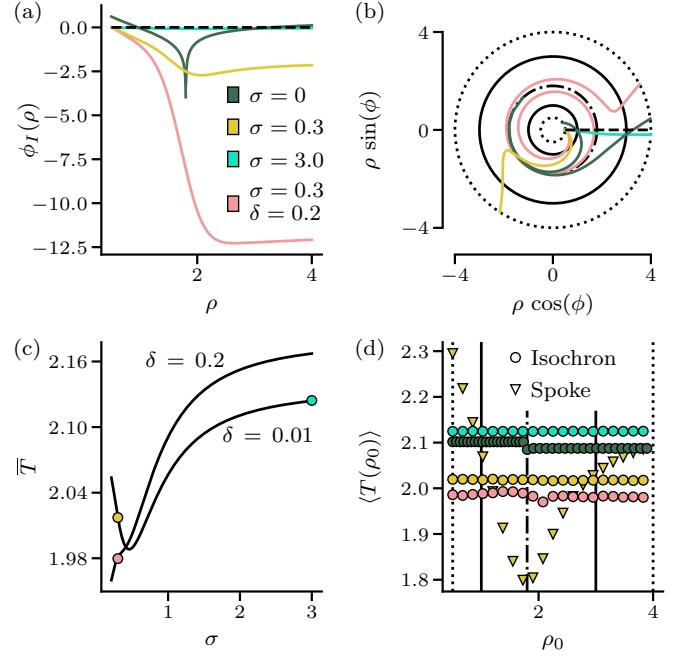


FIG. 2. MRT-Isochrons of the Guckenheimer-Schwabedal-Pikovsky oscillator. Panels as in Fig. 1 but for Eq. (10). Parameters:  $\omega = 3$ ,  $c = 1.8$ ,  $\rho_- = 0.5$ ,  $\rho_+ = 4.0$ .

phase uniquely defines one phase for the entire system. This system is given by

$$\begin{aligned} \dot{\rho} &= \rho(1-\rho)(3-\rho)(c-\rho) + \frac{\sigma^2 \rho}{2} + \sigma \rho \xi(t), \\ \dot{\phi} &= \omega + \delta(\rho-2) - (1-\rho)(3-\rho). \end{aligned} \quad (10)$$

The unstable limit cycle at  $\rho = c$  separates the basins of attraction at  $\rho = 1$  and  $\rho = 3$ . With noise, the unstable limit cycle can be surmounted, smoothing the discontinuity, and thus resulting in one stochastic isochron that is continuous over the whole domain connecting both basins of attraction [see Figs. 2(a) and 2(b)].

While MRTs for a given noise intensity remain constant for initial positions along the corresponding isochron, they vary significantly if the initial set and target line is a ray emanating from the origin [cf. Fig. 2(d)]. For  $D = 0$ , the return time suffers a jump by  $2\delta$  between the basins of attraction (i.e., for an initial point  $\rho = c$ ), reflecting the above-mentioned fact that there is no unique phase for the deterministic system. The stronger this jump is, the more twisted the stochastic MRT isochron becomes (cf. lines for  $\delta = 0.01$  and  $\delta = 0.2$  in Figs. 2(a) and 2(b);  $\delta$  may also change how the mean rotation period depends on the noise level [cf. Fig. 2(c)] We note that for strongly increasing noise, the shape of the isochron flattens as again expected from our general consideration.

### C. A monomial model

According to what we have found so far, we may expect that in the strong-noise limit (until now, the less explored regime of stochastic oscillators), the isochrons always approach a radial spoke [conclusion (iii) above]. This, however,

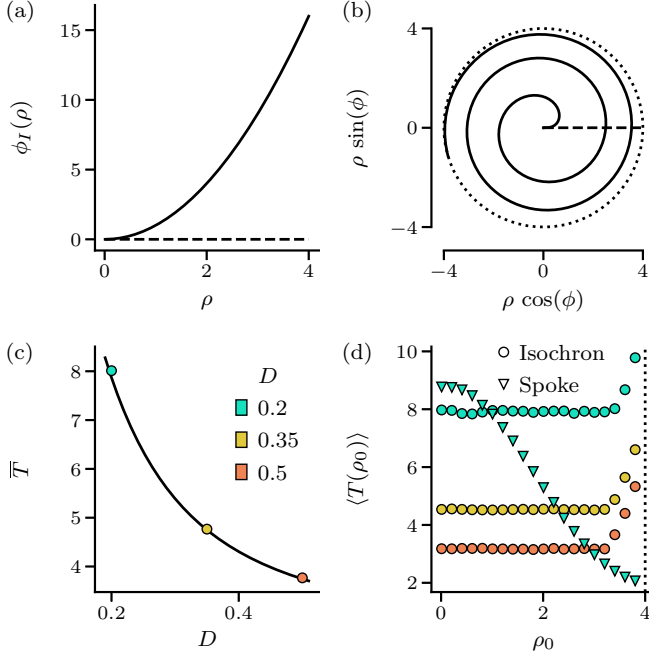


FIG. 3. MRT-isochrons of the monomial model. Presentation in the panels is as in Fig. 1 but for Eq. (11) with  $n = 1$ ,  $\rho_- = 0$ ,  $\rho_+ = \infty$ . Simulations in (d) are, however, performed with  $\rho_- = 10^{-4}$ ,  $\rho_+ = 4.0$  consequently, the MRT property is only obeyed for initial points far from the outer boundary.

is only true for systems with finite boundaries. To show this, we consider a particularly simple model system with monomial frequency dependence, for which the integrals in Eq. (6) can be expressed by elementary functions. The model obeys

$$\begin{aligned} \dot{\rho} &= -\alpha + \frac{D}{\rho} + \sqrt{2D} \xi_\rho(t), \\ \dot{\phi} &= -\beta \rho^n + \frac{\sqrt{2D}}{\rho} \xi_\phi(t), \end{aligned} \quad (11)$$

with positive parameters  $\alpha$ ,  $\beta$  and integer  $n$ , resulting in clockwise rotations with a speed that increases as a power law with increasing radius. We are specifically interested in the limit in which the inner boundary approaches the origin and the outer boundary goes to infinity. In this limit, the MRT and the isochrons can be expressed by elementary functions [21]; particularly simple and striking is the expression for  $n = 1$ :

$$\lim_{\substack{\rho_- \rightarrow 0 \\ \rho_+ \rightarrow \infty \\ \alpha > 0}} \phi(\rho) = \frac{\beta}{\alpha} \frac{\rho^2}{2}, \quad \lim_{\substack{\rho_- \rightarrow 0 \\ \rho_+ \rightarrow \infty \\ \alpha > 0}} \bar{T} = \frac{\alpha}{2\beta D}. \quad (12)$$

Hence, quite surprisingly, the MRT phase is completely independent of the noise level but clearly different from a simple ray [see Figs. 3(a) and 3(b)]. Specifically in the limit  $D \rightarrow \infty$  the isochrons do not converge to the spokes of wheel, which is due to the absence of finite boundaries: for stronger and stronger noise, the main share of probability moves to larger and larger radii and the mean rotation time drops strongly [see Fig. 3(c)].

We can test how important the infinite boundary condition is by running stochastic simulations with initial set and

target line with the isochron Eq. (12) but imposing a reflecting boundary at a finite value  $\rho_+ < \infty$  [for this setting, Eq. (12) is *not* the exact isochron]. For all noise intensities, the MRT is flat as a function of the initial radius except for a finite region close to the outer boundary [see Fig. 3(d)].

#### IV. ISOVARIANCE CURVES

The same approach used for the isochrons permits us to calculate the lines of constant variance, that is, the lines for which the return time to the line after one rotation possesses the same variance irrespective of the starting point. It turns out that these lines are the contour lines of the variance function, obeying

$$\mathcal{L}^\dagger \Delta = q_\rho^2 (\partial_\rho T(\rho, \phi))^2 + q_\phi^2 (\partial_\phi T(\rho, \phi))^2 \quad (13)$$

with a jump condition  $\Delta(\rho, \phi) = \Delta(\rho, \phi + 2\pi) + \bar{\Delta}$  which can be solved for the isotropic oscillator by a similar ansatz  $\Delta(\rho) = \Delta_\rho(\rho) - \phi \bar{\Delta}/(2\pi)$  resulting in the parametrization of the isovariance curve

$$\begin{aligned} \phi_\Delta(\rho) &= 2 \int_{\rho_-}^{\rho} dq \int_{\rho_-}^q du \left[ \frac{2\pi}{\Delta} \left( q_\rho^2(u) (\partial_u T_\rho(u))^2 + \frac{q_\phi^2(u) \bar{T}^2}{4\pi^2} \right) \right. \\ &\quad \left. - f(u) \right] \exp \left( -2 \int_u^q dv \frac{g(v)}{q_\rho^2(v)} \right) / q_\rho^2(u). \end{aligned} \quad (14)$$

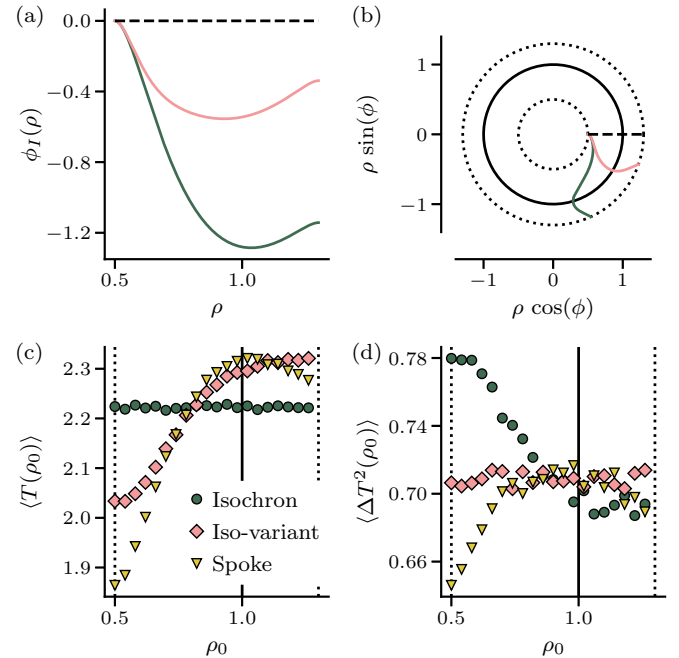


FIG. 4. Isovariance curves for the Newby-Schwemmer oscillator. (a) Isochronal curve and curve of constant return-time variance of the Newby-Schwemmer model in terms of angle variable vs radius. (b) Same curves as in (a), in cartesian coordinates. (c) Mean return time to isochrons, isovariance line, or spoke as function of the initial point on the respective line. (d) Variances of the return times  $\langle \Delta T^2 \rangle$  as function of initial position on the respective lines  $\rho_0$ .



Here the variance of the rotation time  $\bar{\Delta}$  is given by

$$\bar{\Delta} = -2\pi \frac{\int_{\rho_-}^{\rho_+} d\rho \left[ (\partial_\rho T_\rho(\rho))^2 + \frac{q_\rho^2}{q_\phi^2} \frac{\bar{T}^2}{4\pi^2} \right] \exp\left(-2 \int_\rho^{\rho_+} du \frac{g(u)}{q_\rho^2(u)}\right)}{\int_{\rho_-}^{\rho_+} d\rho f(\rho) \exp\left(-2 \int_\rho^{\rho_+} du \frac{g(u)}{q_\rho^2(u)}\right) / q_\rho^2(\rho)}. \quad (15)$$

We have evaluated and tested these formulas for the Newby-Schwemmer oscillator Eq. (9) and also compare the resulting isovariance lines to the isochrons and the spoke of wheel in Fig. 4. We observe that isochron and isovariance curve do not agree in this case: the iso-variance curve [pink line in Figs. 4(a) and 4(b)] is significantly less twisted than the isochron (green line). In panels (c) and (d) we test the defining properties of the two lines: the MRT is approximately independent of the starting point only for the isochron but neither for the isovariance curve nor the spoke (c); the variance of the return time is approximately flat as a function of the starting point for the isovariance line but neither for the isochron nor the spoke.

## V. CONCLUSIONS

We have found the analytical mapping for Schwabedal and Pikovsky's mean return-time (MRT) phase for the important class of planar isotropic stochastic oscillators and have tested it for three examples. We have seen that for systems with finite boundaries, the phase description in the strong noise limit always yields the geometric phase (spokes of a wheel); for small to moderate noise, the curvature of the MRT phase isochrons reflect the stochastic interplay between radial and

angular dynamics. We also demonstrated that constancy of the first cumulant (the MRT) over the isochron does not imply constancy of higher cumulants, for instance, the variance of the return time for different initial positions on the isochron. We could find an equation and solve it for the isovariance curve: in our example the resulting line was quite different from the MRT isochron.

In some applications, it may also be of interest to quantify the correlations between subsequent return times; in neuroscience, for instance, this would be the so-called interspike-interval correlations (see, e.g., Refs. [22–26]). Remarkably, it was shown very recently [27] that return times based on the MRT phase display vanishing correlations. The associated point process defined by the MRT phase is in this respect particularly simple, which is a clear advantage of this phase concept for stochastic oscillators.

We hope that our results can be used to address important open issues in the analysis of stochastic oscillators: (i) the comparison to the asymptotic phase [12] in some analytically tractable cases (see, e.g., Ref. [28]); (ii) the oscillator response to external perturbations via a generalized phase-response curve [29,30]; (iii) the analysis of variability in neuronal firing patterns [19]; (iv) the treatment of networks of strongly stochastic oscillators [31].

- 
- [1] A. Skupin, H. Kettenmann, U. Winkler, M. Wartenberg, H. Sauer, S. C. Tovey, C. W. Taylor, and M. Falcke, How does intracellular  $Ca^{2+}$  oscillate: By chance or by the clock? *Biophys. J.* **94**, 2404 (2008).
  - [2] J. T. Walter, K. Alvina, M. D. Womack, C. Chevez, and K. Khodakhah, Decreases in the precision of Purkinje cell pace-making cause cerebellar dysfunction and ataxia, *Nat. Neurosci.* **9**, 389 (2006).
  - [3] B. McNamara, K. Wiesenfeld, and R. Roy, Observation of Stochastic Resonance in a Ring Laser, *Phys. Rev. Lett.* **60**, 2626 (1988).
  - [4] A. J. McKane and T. J. Newman, Predator-Prey Cycles from Resonant Amplification of Demographic Stochasticity, *Phys. Rev. Lett.* **94**, 218102 (2005).
  - [5] A. T. Winfree, Patterns of phase compromise in biological cycles, *J. Math. Biol.* **1**, 73 (1974).
  - [6] J. Guckenheimer, Isochrons and phaseless sets, *J. Math. Biol.* **1**, 259 (1975).
  - [7] J. A. Freund, A. B. Neiman, and L. Schimansky-Geier, Analytic description of noise-induced phase synchronization, *Europhys. Lett.* **50**, 8 (2000).
  - [8] J. A. Freund, L. Schimansky-Geier, and P. Hänggi, Frequency and phase synchronization in stochastic systems, *Chaos* **13**, 225 (2003).
  - [9] P. Zhou, S. D. Burton, N. Urban, and G. B. Ermentrout, Impact of neuronal heterogeneity on correlated colored-noise-induced synchronization, *Front. Comput. Neurosci.* **7**, 113 (2013).
  - [10] R. Ma, G. S. Klindt, I. H. Riedel-Kruse, F. Jülicher, and B. M. Friedrich, Active Phase and Amplitude Fluctuations of Flagellar Beating, *Phys. Rev. Lett.* **113**, 048101 (2014).
  - [11] J. Schwabedal and A. Pikovsky, Phase Description of Stochastic Oscillations, *Phys. Rev. Lett.* **110**, 204102 (2013).
  - [12] P. J. Thomas and B. Lindner, Asymptotic Phase of Stochastic Oscillators, *Phys. Rev. Lett.* **113**, 254101 (2014).
  - [13] G. Giacomini, C. Poquet, and A. Shapira, Small noise and long time phase diffusion in stochastic limit cycle oscillators, *J. Diff. Equ.* **264**, 1019 (2018).
  - [14] Z. Aminzare, P. P. Holmes, and V. Srivastava, On phase reduction and time period of noisy oscillators, in *Proceedings of the 2019 IEEE 58th Conference on Decision and Control (CDC)* (IEEE, New York, 2019), p. 4717.
  - [15] M. Engel and Ch. Kühn, A random dynamical systems perspective on isochronicity for stochastic oscillations, *Commun. Math. Phys.* **386**, 1603 (2021).
  - [16] A. Pérez-Cervera, B. Lindner, and P. J. Thomas, Isostables for Stochastic Oscillators, *Phys. Rev. Lett.* **127**, 254101 (2021).

- [17] A. Cao, B. Lindner, and P. J. Thomas, A partial differential equation for the mean—first—return-time phase of planar stochastic oscillators, *SIAM J. App. Math.* **80**, 422 (2020).
- [18] C. W. Gardiner, *Handbook of Stochastic Methods* (Springer-Verlag, Berlin, 1985).
- [19] S. Pu and P. J. Thomas, Resolving molecular contributions of ion channel noise to interspike interval variability through stochastic shielding, *Biol. Cybern.* **115**, 267 (2021).
- [20] J. M. Newby and M. A. Schwemmer, Effects of Moderate Noise on a Limit Cycle Oscillator: Counterrotation and Bistability, *Phys. Rev. Lett.* **112**, 114101 (2014).
- [21] K. Holzhausen, An analytic approach to the mean-first-return-time phase of planar isotropic stochastic oscillators, Master's thesis, Humboldt Universität zu Berlin, 2021.
- [22] A. V. Holden, *Models of the Stochastic Activity of Neurons* (Springer-Verlag, Berlin, 1976).
- [23] M. J. Chacron, A. Longtin, M. St-Hilaire, and L. Maler, Suprathreshold Stochastic Firing Dynamics with Memory in P-Type Electoreceptors, *Phys. Rev. Lett.* **85**, 1576 (2000).
- [24] Y. H. Liu and X. J. Wang, Spike-frequency adaptation of a generalized leaky integrate-and-fire model neuron, *J. Comput. Neurosci.* **10**, 25 (2001).
- [25] F. Farkhooi, M. F. Strube-Bloss, and M. P. Nawrot, Serial correlation in neural spike trains: Experimental evidence, stochastic modeling, and single neuron variability, *Phys. Rev. E* **79**, 021905 (2009).
- [26] L. Ramlow and B. Lindner, Interspike interval correlations in neuron models with adaptation and correlated noise, *PLoS Comput. Biol.* **17**, e1009261 (2021).
- [27] K. Holzhausen, L. Ramlow, S. Pu, P. J. Thomas, and B. Lindner, Mean-return-time phase of a stochastic oscillator provides an approximate renewal description for the associated point process, *Biol. Cybern.* **116**, 149 (2022).
- [28] P. J. Thomas and B. Lindner, Phase descriptions of a multidimensional Ornstein-Uhlenbeck process, *Phys. Rev. E* **99**, 062221 (2019).
- [29] R. Galán, G. Ermentrout, and N. Urban, Efficient Estimation of Phase-Resetting Curves in Real Neurons and Its Significance for Neural-Network Modeling, *Phys. Rev. Lett.* **94**, 158101 (2005).
- [30] G. B. Ermentrout, R. F. Galán, and N. N. Urban, Relating Neural Dynamics to Neural Coding, *Phys. Rev. Lett.* **99**, 248103 (2007).
- [31] B. Ermentrout and D. Saunders, Phase resetting and coupling of noisy neural oscillators, *J. Comput. Neurosci.* **20**, 179 (2006).